Compound Heterozygosity for Loss-of-Function Lysyl-tRNA Synthetase Mutations in a Patient with Peripheral Neuropathy

Heather M. McLaughlin,[1] Reiko Sakaguchi,[2] Cuiping Liu,[2] Takao Igarashi,[2] Davut Pehlivan,[3] Kristine Chu,[4] Ram Iyer,[5] Pedro Cruz,[4] Praveen F. Cherukuri,[4] Nancy F. Hansen,[4] James C. Mullikin,[4,6] NISC Comparative Sequencing Program,[6] Leslie G. Biesecker,[7] Thomas E. Wilson,[1,5] Victor Ionasescu,[8] Garth Nicholson,[9,10] Charles Searby,[8] Kevin Talbot,[11] Jeffrey M. Vance,[12] Stephan Züchner,[12] Kinga Szigeti,[3,13] James R. Lupski,[3,14,15] Ya-Ming Hou,[2] Eric D. Green,[4,6] and Anthony Antonellis[1,16,*]

Charcot-Marie-Tooth (CMT) disease comprises a genetically and clinically heterogeneous group of peripheral nerve disorders characterized by impaired distal motor and sensory function. Mutations in three genes encoding aminoacyl-tRNA synthetases (ARSs) have been implicated in CMT disease primarily associated with an axonal pathology. ARSs are ubiquitously expressed, essential enzymes responsible for charging tRNA molecules with their cognate amino acids. To further explore the role of ARSs in CMT disease, we performed a large-scale mutation screen of the 37 human ARS genes in a cohort of 355 patients with a phenotype consistent with CMT. Here we describe three variants (p.Leu133His, p.Tyr173SerfsX7, and p.Ile302Met) in the lysyl-tRNA synthetase (*KARS*) gene in two patients from this cohort. Functional analyses revealed that two of these mutations (p.Leu133His and p.Tyr173SerfsX7) severely affect enzyme activity. Interestingly, both functional variants were found in a single patient with CMT disease and additional neurological and non-neurological sequelae. Based on these data, *KARS* becomes the fourth ARS gene associated with CMT disease, indicating that this family of enzymes is specifically critical for axon function.

Charcot-Marie-Tooth (CMT) disease represents a genetically and clinically heterogeneous group of peripheral neuropathies, with a prevalence of 1 in 2500 individuals.[1] The major clinical features of CMT include distal muscular weakness and wasting, impaired sensation, steppage gait, pes cavus, and diminished deep-tendon reflexes.[2,3] Broadly, CMT can be subdivided into two classes according to electrophysiological criteria.[2] In CMT1, patients exhibit decreased motor nerve conduction velocities (MNCVs) and demyelination of peripheral nerve axons. In CMT2, patients do not show primary demyelination but do exhibit axonal loss accompanied by decreased amplitudes of evoked nerve responses.

Aminoacyl-tRNA synthetases (ARSs) are a ubiquitously expressed, essential family of enzymes responsible for charging tRNA molecules with their cognate amino acids in the cytoplasm and mitochondria.[4] Interestingly, mutations in three genes encoding aminoacyl-tRNA synthetases have been implicated in CMT disease characterized by an axonal pathology: glycyl- (*GARS* [MIM 601472]), tyrosyl- (*YARS* [MIM 608323]), and alanyl- (*AARS* [MIM 613287]) tRNA synthetase.[5–7] Although the molecular pathology of axonopathy associated with ARS mutations remains unclear, several mutant forms of GARS and YARS impair tRNA charging, cell viability in yeast assays, and cellular localization in mammalian cells, suggesting that impaired enzyme function may play a role in disease onset, with neurons harboring very long axons more susceptible to tRNA charging deficits.[7,8] Combined, these findings strongly suggest that all genes encoding an ARS are excellent candidates for CMT disease. We therefore carried out a sequencing-based mutation screen of the 37 ARS genes in a cohort of 355 patients with a phenotype consistent with CMT and no known disease-causing mutation. The appropriate, institute-specific review boards approved all studies performed herein, and informed consent was obtained from all subjects. This study revealed four protein-coding variants (including one previously described polymorphism) in the lysyl-tRNA synthetase (*KARS* [MIM 601421]) gene. *KARS* resides on chromosome

[1]Department of Human Genetics, University of Michigan Medical School, Ann Arbor, MI 48109, USA; [2]Department of Biochemistry and Molecular Pharmacology, Thomas Jefferson University, Philadelphia, PA 19107, USA; [3]Department of Molecular and Human Genetics, Baylor College of Medicine, Houston, TX 77030, USA; [4]Genome Technology Branch, National Human Genome Research Institute, National Institutes of Health (NIH), Bethesda, MD 20892, USA; [5]Department of Pathology, University of Michigan Medical School, Ann Arbor, MI 48109, USA; [6]NIH Intramural Sequencing Center (NISC), National Human Genome Research Institute, National Institutes of Health, Bethesda, MD 20892, USA; [7]Genetic Disease Research Branch, National Human Genome Research Institute, National Institutes of Health, Bethesda, MD 20892, USA; [8]Division of Medical Genetics, Department of Pediatrics, University of Iowa, Iowa City, IA 52242, USA; [9]Northcott Neuroscience Laboratory, ANZAC Research Institute and Molecular Medicine Laboratory, Concord Hospital, Concord, New South Wales 2139, Australia; [10]Faculty of Medicine, University of Sydney, Camperdown, New South Wales 2006, Australia; [11]Department of Clinical Neurology, University of Oxford, OX1 3QX Oxford, UK; [12]Hussman Institute for Human Genomics, University of Miami Miller School of Medicine, Miami, FL 33136, USA; [13]Department of Neurology, Baylor College of Medicine, Houston, TX 77030, USA; [14]Department of Pediatrics, Baylor College of Medicine, Houston, TX 77030, USA; [15]Texas Children's Hospital, Houston, TX 77030, USA; [16]Department of Neurology, University of Michigan Medical School, Ann Arbor, MI 48109, USA

*Correspondence: antonell@umich.edu

DOI 10.1016/j.ajhg.2010.09.008.

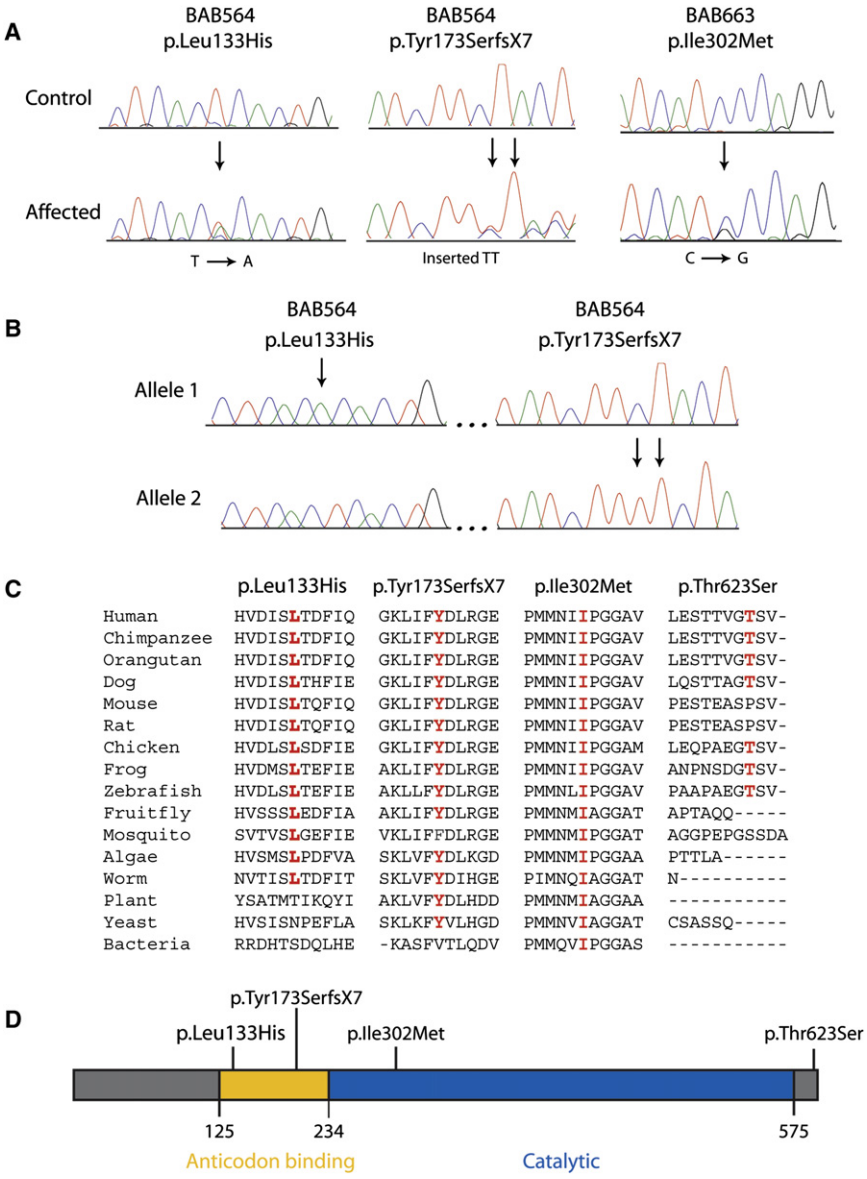

Figure 1. Characterization, Conservation, and Localization of *KARS* Variants
(A) Representative sections of sequence chromatograms are shown for the regions encompassing each identified *KARS* variant in the indicated individuals. Arrows denote the variant (present in the heterozygous state), with the predicted amino acid changes depicted above.
(B) Chromatograms from allele-specific sequencing of an ~3.7 kb PCR-generated genomic segment spanning the two *KARS* variants (p.Leu133His and p.Tyr173SerfsX7) identified in patient BAB564. Arrows indicate each mutation. Note that each variant was identified on separate alleles, indicating that this patient is a compound heterozygote.
(C) For each of the four detected variants, the affected amino acid is shown along with the flanking KARS protein sequence in multiple, evolutionarily diverse species. Note that each specific amino acid change is given at the top, with the relevant position depicted in red for each protein sequence. Dashes indicate gaps in the sequence alignment.
(D) The known functional domains of the KARS protein are indicated in yellow ($tRNA^{Lys}$-binding domain) and blue (core catalytic domain).

16q23.1 and encodes the enzyme responsible for charging $tRNA^{Lys}$ molecules. Importantly, *KARS* is the only locus in the human genome encoding an enzyme responsible for $tRNA^{Lys}$ charging and is required in both the cytoplasm and mitochondria for protein translation.[9]

One *KARS* variant was identified in the heterozygous state in patient BAB663 (Figure 1A; BAB663): c.906C>G, which predicts p.Ile302Met. This patient's pedigree indicates an apparent autosomal-dominant mode of inheritance (see Figure S1 available online). Electrophysiological studies revealed that BAB663 exhibited normal MNCVs in all nerves tested, accompanied by normal amplitudes of evoked nerve response (6 mV, 7 mV, 8 mV, 11 mV, 7 mV, and 4 mV in the left median, left ulnar, right median, right ulnar, left peroneal, and left post-tibial nerves, respectively). Distal motor latencies were prolonged (7.2 ms in the right and left median nerves, 3.6 ms in the left ulnar nerve, 4.2 ms in the left ulnar nerve, 7.6 ms in the left peroneal nerve, and 5.8 ms in the left tibial nerve). Thus, this patient has a phenotype consistent with hereditary neuropathy, with liability to pressure palsies (HNPP [MIM 162500]).[10]

Two additional *KARS* variants were identified in a patient with intermediate CMT, developmental delay, self-abusive behavior, dysmorphic features, and vestibular Schwannoma (Figure 1A; BAB564): c.398T>A, which predicts p.Leu133His, and c.524_525insTT, which predicts a frameshift mutation p.Tyr173SerfsX7. BAB564 exhibited MNCVs of 39.5 m/s and 30.6 m/s in the median and ulnar nerves, consistent with an intermediate CMT phenotype.[11] In addition, this patient displayed decreased amplitudes of evoked motor response in these nerves (0.5 mV). More detailed molecular analysis of BAB564 (involving PCR amplification, cloning, and sequencing the ~3.7 kb segment encompassing the two detected variants) revealed that this individual is a compound heterozygote for p.Leu133His and p.Tyr173SerfsX7 (Figure 1B). Because this individual was adopted, these efforts were critical for distinguishing between a complex allele and compound heterozygosity (DNA samples from the biological parents are unavailable). Finally, p.Thr623Ser was identified in 31 out of 710 chromosomes studied (frequency = 0.044). This variant is present in dbSNP (rs6834), indicating that p.Thr623Ser represents a rare polymorphism.

Table 1. ARS Missense Variants Identified in Patients BAB564 and BAB663

BAB564				BAB663			
Gene	**MIM**	**Variant**	**Notes**	**Gene**	**MIM**	**Variant**	**Notes**
EPRS	138295	p.Asp308Glu	rs2230301[1]	*EPRS*	138295	p.Asp308Glu	rs2230301[1]
FARS2	611592	p.Asn280Ser	rs11243011[1]	*FARSB*	609690	p.Val585Ile	rs7185[1]
FARSB	609690	p.Val585Ile	rs7185[1]	*IARS*	600709	p.Lys1182Glu	rs556155[1]
KARS	601421	p.Leu133His	This study	*KARS*	601421	p.Ile302Met	This study
RARS	107820	p.Val3Ile	rs244903[1]	*NARS*	108410	p.Asn218Ser	2/710[2]
RARS	107820	p.Phe397Tyr	rs2305734[1]	*RARS*	107820	p.Val3Ile	rs244903[1]
TARS	187790	p.Ala95Glu	1/710[2,3]	*YARS2*	610957	p.Glu191Val	10/710[2]

[1] dbSNP accession number.
[2] Number of chromosomes identified in total patient cohort.
[3] Does not affect TARS enzyme function in aminoacylation assays (Jiqiang Ling and Dieter Söll, personal communication).

Samples from patients BAB663 and BAB564 were screened for mutations in other genes previously implicated in CMT disease, including the CMT1A duplication and point mutations in *AARS*, *EGR2* (MIM 129010), *GARS*, *GDAP1* (MIM 606598), *GJB1* (MIM 304040), *MPZ* (MIM 159440), *NEFL* (MIM 162280), *PMP22* (MIM 601097), *PRX* (MIM 605725), *SIMPLE* (MIM 603795), *SOX10* (MIM 602229), *LMNA* (MIM 150330), *TDP1* (MIM 607198), *MTMR2* (MIM 603557), and *YARS*. Patient BAB663 is heterozygous for p.Arg238His *GJB1*,[12] p.Thr87Thr *SIMPLE*,[13] and the 1.4 Mb *PMP22* deletion.[14] Interestingly, the *PMP22* deletion and p.Arg238His *GJB1* variant have previously been reported as pathogenic in HNPP and CMTX1 (MIM 302800), respectively.[14,15] No mutations or copy number variations were detected in patient BAB564. Importantly, this includes *MPZ* and *YARS*, both of which have been associated with intermediate CMT.[16] To further exclude known causes of intermediate CMT, we screened BAB564 for *DNM2* (MIM 602378) mutations; these studies were also negative. Thus, BAB564 does not carry mutations in genes previously implicated in intermediate CMT.[11,16] Finally, six variants in other ARS genes were identified in each individual, although none are likely to be pathogenic (Table 1).

To determine whether the *KARS* variants are benign, we performed appropriate genotyping assays on DNA samples from neurologically normal controls of European decent (NINDS/Coriell). The p.Leu133His, p.Ile302Met, and p.Tyr173SerfsX7 variants were not detected in 1036, 1094, and 1098 chromosomes tested, respectively. We also screened all *KARS* protein-coding sequences for mutations in 95 individuals from the ClinSeq cohort.[17] The only protein-coding variant identified was p.Thr623Ser, which occurred in 11 out of 190 chromosomes (frequency = 0.058).

The evolutionary conservation of each affected KARS residue was assessed by aligning protein sequences from KARS orthologs from multiple species (Figure 1C). Leucine 133 was conserved among all species analyzed, with the exception of plant, yeast, and bacteria. Isoleucine 302 was conserved among all species examined, including yeast and bacteria. Tyrosine 173 was conserved among all species analyzed, with the exception of mosquito and bacteria. In contrast, threonine 623 was not conserved between human and rodents and resides in a region that does not align with protein sequences from nonvertebrate species. Thus, the three rare *KARS* variants identified in our patient cohort reside at remarkably well-conserved amino acids, suggesting that they have a potential functional impact on the KARS protein.

We further computationally predicted the effect of each variant on protein function with the MuPro, PolyPhen, PolyPhen2, SIFT, Align GVGD, and CDPred algorithms (Table 2).[18–23] It is notable that each of the known disease-associated *GARS*, *YARS*, and *AARS* mutations is predicted to be pathogenic by at least three of these six algorithms (Table 2). The p.Leu133His and p.Ile302Met *KARS* variants are predicted to interfere with protein function by four and three of the six algorithms, respectively. The p.Tyr173SerfsX7 *KARS* variant could not be analyzed, because these algorithms are unable to predict the effect of frameshift mutations; however, this variant is predicted to represent a null allele via nonsense-mediated decay. Importantly, the p.Thr623Ser polymorphism was predicted to be pathogenic by only one of the six algorithms.

The KARS holoenzyme exists in dimeric and tetrameric forms.[24] We mapped each affected KARS residue onto the crystal structure of the human enzyme to examine the amino acid position and structural relationship to functional domains that could potentially alter enzyme function. Leucine 133 is located within an N-terminal anticodon-binding domain (Figure 1D) and is adjacent to the dimer-dimer interface (Figures 2A–2C). This interface may be involved in interactions between KARS and various binding partners, including p38 (MIM 600859) in the mammalian multisynthetase complex, the HIV-1 Gap protein, and mutant forms of SOD1 (MIM 147450) found in patients with amyotrophic lateral sclerosis (MIM 105400).[24–26] The p.Leu133His mutation is likely to impact some of these interactions. The p.Tyr173SerfsX7 variant

Table 2. Computational Predictions of *KARS* Variant Pathogenicity

Gene	Variant	MUPro[1]	PolyPhen[2]	PolyPhen2[3]	SIFT[4]	Align GVGD[5]	CDPred[6]
GARS	p.Glu71Gly	SVM = −1.00[7]	2.21[7]	0.99[7]	0.01[7]	C65[7]	−7[7]
GARS	p.Leu129Pro	SVM = −1.00[7]	2.21[7]	1.00[7]	0.00[7]	C65[7]	−8[7]
GARS	p.Gly240Arg	SVM = 0.30	2.31[7]	0.99[7]	0.00[7]	C65[7]	−8[7]
GARS	p.Gly526Arg	SVM = 0.00	2.79[7]	1.00[7]	0.00[7]	C65[7]	−11[7]
YARS	p.Gly41Arg	SVM = 0.84	2.49[7]	1.00[7]	0.00[7]	C65[7]	−12[7]
YARS	p.Glu196Lys	SVM = −1.00[7]	0.63	0.99[7]	0.17	C55[7]	−2
AARS	p.Arg329His	SVM = −0.77[7]	3.04[7]	1.00[7]	0.00[7]	C25	−10[7]
KARS	p.Leu133His	SVM = −0.61[7]	0.11	0.99[7]	0.06	C65[7]	−4[7]
KARS	p.Ile302Met	SVM = −0.86[7]	0.63	0.36	0.11	C55[7]	−6[7]
KARS	p.Thr623Ser	SVM = −0.62[7]	1.20	0.01	0.25	C0	+1

[1] Support Vector Machine (SVM) scores < 0 indicate a decrease in protein stability.
[2] PolyPhen scores ≥ 1.5 indicate a prediction of pathogenic.
[3] PolyPhen2 scores of ~1 indicate a prediction of pathogenic.
[4] SIFT scores ≤ 0.05 indicate a prediction of pathogenic.
[5] Grantham variation (GV) and Grantham difference (GD) classes $\geq$ C55 indicate a prediction of pathogenic.
[6] CDPred delta scores ≤ -3 indicate a prediction of pathogenic.
[7] Denotes a pathogenic prediction.

resides in the anticodon-binding domain (Figure 1D) and predicts a complete loss of the catalytic domain. Isoleucine 302 resides in the catalytic domain (Figure 1D) and is also adjacent to the dimer-dimer interface (Figures 2A–2C). Thus, p.Ile302Met may also affect the association between KARS and binding partners. Threonine 623 is unresolved in the crystal structure. Importantly, these analyses reveal similarities between p.Leu133His and p.Ile302Met *KARS* and disease-associated *GARS* mutations; most *GARS* mutations affect residues that reside on the dimer interface of the holoenzyme.[27]

KARS catalyzes the aminoacylation of $tRNA^{Lys}$ in the cytoplasm and mitochondria via a two-step aminoacylation reaction.[28] Importantly, 7 out of 10 disease-associated *GARS* and *YARS* mutations tested to date impair aminoacylation activity.[4] We investigated the ability of each KARS variant to catalyze the aminoacylation reaction in vitro. Human cytoplasmic $tRNA^{Lys}$ was synthesized by in vitro transcription and was used as the substrate for aminoacylation. Analysis of the catalytic efficiency (k_{cat}/K_m) of aminoacylation showed that the p.Thr623Ser and p.Ile302Met variants maintain normal catalytic activity, indicating that these variants do not negatively affect aminoacylation. In contrast, p.Leu133His severely impairs enzyme activity, resulting in an ~94% loss of catalytic efficiency of aminoacylation relative to wild-type KARS (Table 3; Figure 2D).

Many *GARS* and *YARS* mutations do not complement deletion of the corresponding yeast orthologs.[7,8] To further assess for defects in KARS enzyme function, we modeled each *KARS* variant in the yeast ortholog (*KRS1*; Table 4) and determined the effect on yeast cell viability via complementation assays. A haploid yeast strain with the endogenous *KRS1* deleted (*krs1*Δ) was maintained via transformation with a wild-type copy of *KRS1* on a *URA3*-bearing vector (pRS316). Experimental alleles were generated on a *LEU2*-bearing vector (pRS315) and transformed into the above strain, and their viability was assessed by analysis of growth on 5-fluoroorotic acid (5-FOA). Wild-type *KRS1* vector supported significant growth, whereas an insert-free pRS315 construct did not (Figure 2E), consistent with our experimental vector harboring functional *KRS1* and with *KRS1* being an essential gene, respectively. The p.Asn103His and p.Ile277Met *KRS1* variants allowed growth in a manner consistent with wild-type *KRS1*. In contrast, p.His146PhefsX12 *KRS1* could not complement the *krs1*Δ allele (Figure 2E), consistent with p.Tyr173SerfsX7 *KARS* representing a null allele.

In summary, we report three rare *KARS* variants in two patients with peripheral neuropathy. The p.Ile302Met variant was discovered in the heterozygous state in an individual with clinical electrophysiological evidence for HNPP and was molecularly found to harbor the common 1.4 Mb deletion, including *PMP22*. Although p.Ile302Met resides at a residue within the catalytic core of the enzyme that is conserved between human and bacteria, we were unable to show an effect on enzyme function via aminoacylation and yeast growth assays. Thus, the *PMP22* deletion should be considered the primary pathogenic mutation in BAB663. However, it will be important to determine whether or not the *PMP22* deletion, p.Arg238His *GJB1*, and p.Ile302Met *KARS* interact to modify the phenotype in this patient; several recent studies suggest the potential for a more severe neuropathy phenotype associated with variants at more than one CMT locus.[29–31]

The p.Leu133His and p.Tyr173SerfsX7 variants were identified in the compound heterozygous state in a patient

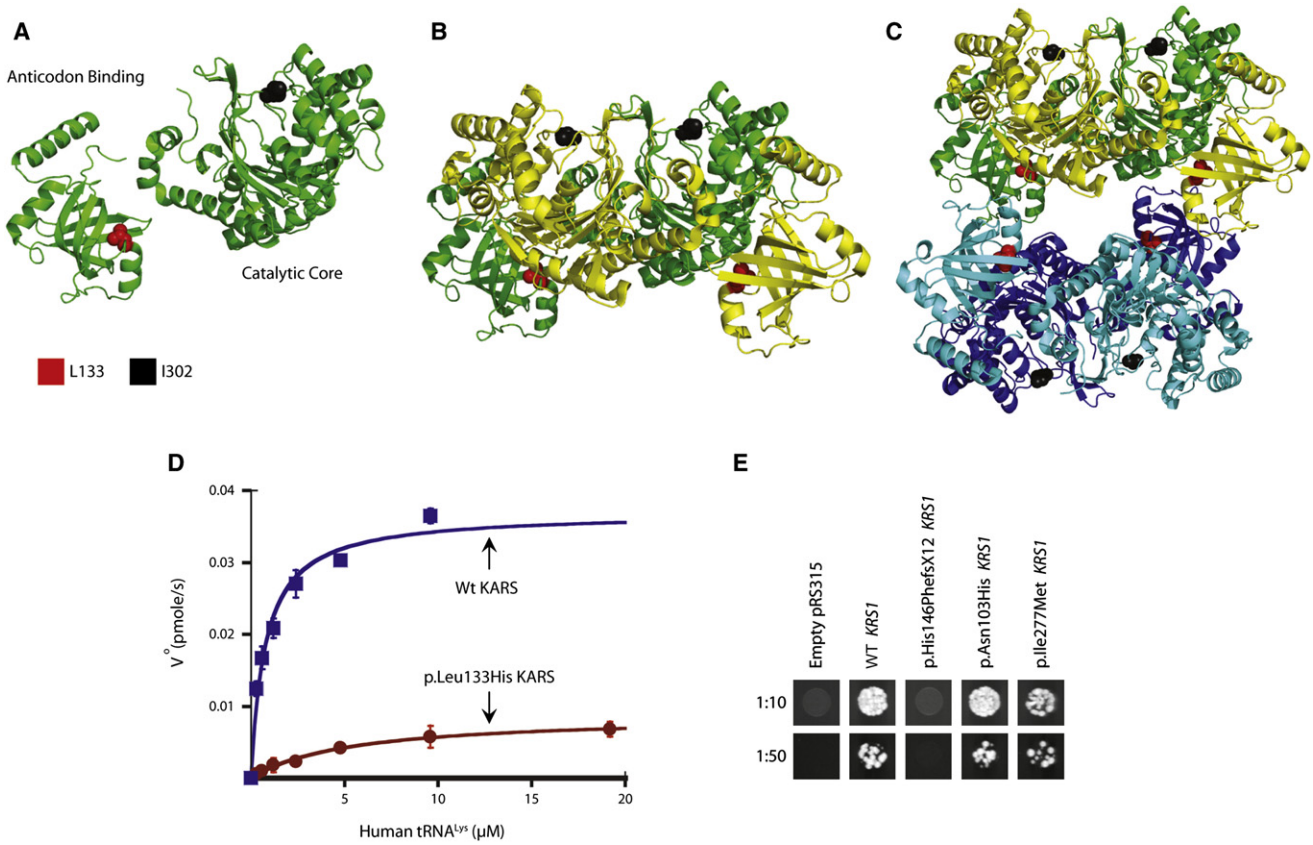

Figure 2. Functional Consequences of *KARS* Variants
(A–C) An illustration of the KARS protein crystal structure is shown for the monomer (A), dimer (B), and tetramer (C). The anti-codon binding and catalytic domains are indicated in (A). The position of residues L133 and I302 are indicated in red and black, respectively. Note that L133 resides at the tetramer interface in (C).
(D) Initial aminoacylation rates, V_0 (pmol/s), of wild-type KARS (blue squares) and p.Leu133His KARS (red circles) were plotted against tRNA concentration and fit to the Michaelis-Menten equation. Error bars indicate standard deviation.
(E) Representative cultures of the indicated yeast strains were inoculated and grown on solid growth medium containing 5-FOA. Each strain was previously transfected with a vector containing no insert (pRS315), wild-type *KRS1* (WT *KRS1*), or the indicated mutant form of *KRS1* that modeled a human *KARS* mutation (see Table 4). Before inoculating on 5-FOA-containing medium, each strain was diluted 1:10 or 1:50 in water.

with intermediate CMT, developmental delay, self-abusive behavior, dysmorphic features, and vestibular Schwannoma. The p.Tyr173SerfsX7 variant represents a loss-of-function allele, and p.Leu133His represents a severely hypomorphic allele in yeast growth and aminoacylation assays, respectively. Combined, these data indicate that the patient has a severe depletion of charged $tRNA^{Lys}$ in both the cytoplasm and mitochondria. It is important to consider these loss-of-function mutations in the context of the CMT and non-CMT phenotypes observed in this patient. To date, three ARS genes have been implicated in CMT.[5–7] The encoded enzymes either are bifunctional (GARS charges tRNA in both the cytoplasm and mitochondria) or charge tRNA in the cytoplasm (YARS and AARS). In each case, the phenotypes are dominant and the mutations are missense or in-frame deletions. Furthermore, each mutation has been associated with a loss of function, as observed by impaired tRNA charging, inability to

Table 3. Enzyme Kinetics of Variant KARS Proteins in Aminoacylation Assays

KARS Enzyme	K_m (μM)	k_{cat} (s^{-1})	k_{cat}/K_m ($s^{-1}\mu M^{-1}$)	Relative Activity
Wild-type	1.8 ± 0.9	1.4 ± 0.1	0.8	1
p.Leu133His	5.8 ± 2.4	0.3 ± 0.3	0.05	0.06
p.Ile302Met	2.1 ± 0.8	2.7 ± 1.6	1.3	1.6
p.Thr623Ser	3.5 ± 0.1	4.0 ± 0.7	1.1	1.4

Table 4. Human KARS Variants Modeled in the Yeast Ortholog KRS1

Human KARS[1]	Yeast KRS1[2]
p.Leu133His	p.Asn103His
p.Tyr173SerfsX7	p.His146PhefsX12
p.Ile302Met	p.Ile277Met

[1] Amino acid coordinates correspond to GenBank accession number NP_001123561.1.
[2] Amino acid coordinates correspond to GenBank accession number NP_010322.1.

complement the deletion of the yeast ortholog, and/or reduced localization of the ARS enzyme to axons.[5,7,8,27] Because haploinsufficiency for *Gars* does not cause a CMT-like phenotype in mouse,[32] a dominant-negative effect has been proposed.[4] Such an effect would reduce tRNA charging levels to ~25%, a level that may breach a threshold required by neurons with particularly long axons.[6] Our functional analyses suggest that KARS charging activity is reduced to well below 25% (~6%) in patient BAB564. As such, compound heterozygosity for a null and severely hypomorphic *KARS* allele may be expected to cause a more severe or complex phenotype than heterozygosity for a dominant-negative ARS mutation. It is also possible that additional genetic complexities could be associated with the non-CMT sequelae—in particular, the vestibular Schwannoma often associated with *NF2* mutations (MIM 607379).[33] Therefore, detailed analysis in a vertebrate model system will be required to tease out the contribution of each *KARS* allele to the neuronal and non-neuronal phenotypes observed in patient BAB564.

The studies presented here describe the fourth association between ARS gene mutations and CMT and outline the importance of using informative and relevant functional assays as a follow-up to large-scale mutation screens. Indeed, our efforts illustrate some of the issues common to contemporary human genetics and genomics; for example, although we have the capacity to sequence large cohorts of patients, the analysis of small families and sporadic cases is often key for assessing the role of specific genes in human disease. In these and other "gene discovery" cases, relevant and informative functional assays provide critical evidence for the pathogenicity of uncharacterized variants.

KARS protein orthologs from multiple species were derived from the following GenBank accession numbers: human (*Homo sapiens*, NP_00112356), chimpanzee (*Pan troglodytes*, XP_511115.2), orangutan (*Pongo abelii*, NP_001123561), dog (*Canis familiaris*, XP_536777.2), mouse (*Mus musculus*, NP_444322), rat (*Rattus norvegicus*, NP_001006968), chicken (*Gallus gallus*, NP_001025754), frog (*Xenopus laevis*, NP_001080633), zebrafish (*Danio rerio*, NP_001002386), fruitfly (*Drosophila melanogaster*, NP_572573), mosquito (*Anopheles gambiae*, XP_310792), algae (*Chlamydomonas reinhardtii*, XP_001697493), worm (*Caenorhabditis elegans*, NP_495454), plant (*Arabidopsis thaliana*, NP_187777), yeast (*Saccharomyces cerevisiae*, NP_010322), bacteria (*Escherichia sp.* 1_1_43, ZP_04871218).

Supplemental Data

Supplemental Data include one figure and can be found with this article online at http://www.cell.com/AJHG/.

Acknowledgments

We are indebted to the patients and their families for their participation in this study. We thank Ellen Pederson, Bob Lyons, and the University of Michigan DNA Sequencing Core for sequencing and genotyping assistance, Jeffrey Innis and the Michigan Medical Genetics Laboratory for anonymized DNA samples, Giovanni Manfredi and Kiyotaka Shiba for *KARS* cDNA constructs, and Jiqiang Ling and Dieter Söll for sharing unpublished data. We are also very grateful to the two anonymous reviewers for their helpful comments and suggestions, which dramatically improved the study. This work was supported in part by grant R00NS060983 from the National Institute of Neurological Diseases and Stroke (AA) and by the Intramural Research Program of the National Human Genome Research Institute (NIH). The ClinSeq cohort and sequencing were also supported by Intramural Funding from the National Human Genome Research Institute. H.M.M. was supported by the Rackham Merit Fellowship and the NIH Genetics Training Grant T32 GM007544-32. Y.-M.H. and R.S. were supported by a grant from the Muscular Dystrophy Association (157681 to Y.-M.H.).

Received: July 10, 2010
Revised: September 1, 2010
Accepted: September 15, 2010
Published online: October 7, 2010

Web Resources

The URLs for data presented herein are as follows:

Align GVGD, http://agvgd.iarc.fr/agvgd_input.php
ClustalW2, http://www.ebi.ac.uk/Tools/clustalw2/index.html
Conserved Domain-Based Prediction (CDPred), http://research.nhgri.nih.gov/software/CDPred/
MUpro: Prediction of Protein Stability Changes for Single-Site Mutations from Sequences, http://www.ics.uci.edu/~baldig/mutation.html
Online Mendelian Inheritance in Man (OMIM), http://www.ncbi.nlm.nih.gov/Omim/
PolyPhen, http://genetics.bwh.harvard.edu/pph/index.html
PolyPhen-2, http://genetics.bwh.harvard.edu/pph2/
SIFT Sequence, http://sift.jcvi.org/www/SIFT_seq_submit2.html

References

1. Skre, H. (1974). Genetic and clinical aspects of Charcot-Marie-Tooth's disease. Clin. Genet. *6*, 98–118.
2. Dyck, P.J., and Lambert, E.H. (1968). Lower motor and primary sensory neuron diseases with peroneal muscular atrophy. II. Neurologic, genetic, and electrophysiologic findings in various neuronal degenerations. Arch. Neurol. *18*, 619–625.
3. Murakami, T., Garcia, C.A., Reiter, L.T., and Lupski, J.R. (1996). Charcot-Marie-Tooth disease and related inherited neuropathies. Medicine (Baltimore) *75*, 233–250.
4. Antonellis, A., and Green, E.D. (2008). The role of aminoacyl-tRNA synthetases in genetic diseases. Annu. Rev. Genomics Hum. Genet. *9*, 87–107.
5. Latour, P., Thauvin-Robinet, C., Baudelet-Méry, C., Soichot, P., Cusin, V., Faivre, L., Locatelli, M.C., Mayençon, M., Sarcey, A., Broussolle, E., et al. (2010). A major determinant for binding and aminoacylation of tRNA(Ala) in cytoplasmic Alanyl-tRNA synthetase is mutated in dominant axonal Charcot-Marie-Tooth disease. Am. J. Hum. Genet. *86*, 77–82.
6. Antonellis, A., Ellsworth, R.E., Sambuughin, N., Puls, I., Abel, A., Lee-Lin, S.Q., Jordanova, A., Kremensky, I., Christodoulou, K., Middleton, L.T., et al. (2003). Glycyl tRNA synthetase mutations

in Charcot-Marie-Tooth disease type 2D and distal spinal muscular atrophy type V. Am. J. Hum. Genet. *72*, 1293–1299.
7. Jordanova, A., Irobi, J., Thomas, F.P., Van Dijck, P., Meerschaert, K., Dewil, M., Dierick, I., Jacobs, A., De Vriendt, E., Guergueltcheva, V., et al. (2006). Disrupted function and axonal distribution of mutant tyrosyl-tRNA synthetase in dominant intermediate Charcot-Marie-Tooth neuropathy. Nat. Genet. *38*, 197–202.
8. Antonellis, A., Lee-Lin, S.Q., Wasterlain, A., Leo, P., Quezado, M., Goldfarb, L.G., Myung, K., Burgess, S., Fischbeck, K.H., and Green, E.D. (2006). Functional analyses of glycyl-tRNA synthetase mutations suggest a key role for tRNA-charging enzymes in peripheral axons. J. Neurosci. *26*, 10397–10406.
9. Tolkunova, E., Park, H., Xia, J., King, M.P., and Davidson, E. (2000). The human lysyl-tRNA synthetase gene encodes both the cytoplasmic and mitochondrial enzymes by means of an unusual alternative splicing of the primary transcript. J. Biol. Chem. *275*, 35063–35069.
10. Li, J., Krajewski, K., Shy, M.E., and Lewis, R.A. (2002). Hereditary neuropathy with liability to pressure palsy: The electrophysiology fits the name. Neurology *58*, 1769–1773.
11. Nicholson, G., and Myers, S. (2006). Intermediate forms of Charcot-Marie-Tooth neuropathy: A review. Neuromolecular Med. *8*, 123–130.
12. Bergoffen, J., Scherer, S.S., Wang, S., Scott, M.O., Bone, L.J., Paul, D.L., Chen, K., Lensch, M.W., Chance, P.F., and Fischbeck, K.H. (1993). Connexin mutations in X-linked Charcot-Marie-Tooth disease. Science *262*, 2039–2042.
13. Street, V.A., Bennett, C.L., Goldy, J.D., Shirk, A.J., Kleopa, K.A., Tempel, B.L., Lipe, H.P., Scherer, S.S., Bird, T.D., and Chance, P.F. (2003). Mutation of a putative protein degradation gene LITAF/SIMPLE in Charcot-Marie-Tooth disease 1C. Neurology *60*, 22–26.
14. Chance, P.F., Alderson, M.K., Leppig, K.A., Lensch, M.W., Matsunami, N., Smith, B., Swanson, P.D., Odelberg, S.J., Disteche, C.M., and Bird, T.D. (1993). DNA deletion associated with hereditary neuropathy with liability to pressure palsies. Cell *72*, 143–151.
15. Nelis, E., Simokovic, S., Timmerman, V., Löfgren, A., Backhovens, H., De Jonghe, P., Martin, J.J., and Van Broeckhoven, C. (1997). Mutation analysis of the connexin 32 (Cx32) gene in Charcot-Marie-Tooth neuropathy type 1: Identification of five new mutations. Hum. Mutat. *9*, 47–52.
16. Reilly, M.M. (2007). Sorting out the inherited neuropathies. Pract. Neurol. *7*, 93–105.
17. Biesecker, L.G., Mullikin, J.C., Facio, F.M., Turner, C., Cherukuri, P.F., Blakesley, R.W., Bouffard, G.G., Chines, P.S., Cruz, P., Hansen, N.F., et al; NISC Comparative Sequencing Program. (2009). The ClinSeq Project: Piloting large-scale genome sequencing for research in genomic medicine. Genome Res. *19*, 1665–1674.
18. Adzhubei, I.A., Schmidt, S., Peshkin, L., Ramensky, V.E., Gerasimova, A., Bork, P., Kondrashov, A.S., and Sunyaev, S.R. (2010). A method and server for predicting damaging missense mutations. Nat. Methods *7*, 248–249.
19. Cheng, J., Randall, A., and Baldi, P. (2006). Prediction of protein stability changes for single-site mutations using support vector machines. Proteins *62*, 1125–1132.
20. Johnston, J.J., Teer, J.K., Cherukuri, P.F., Hansen, N.F., Loftus, S.K., Chong, K., Mullikin, J.C., and Biesecker, L.G.; NIH Intramural Sequencing Center. (2010). Massively parallel sequencing of exons on the X chromosome identifies RBM10 as the gene that causes a syndromic form of cleft palate. Am. J. Hum. Genet. *86*, 743–748.
21. Mathe, E., Olivier, M., Kato, S., Ishioka, C., Hainaut, P., and Tavtigian, S.V. (2006). Computational approaches for predicting the biological effect of p53 missense mutations: A comparison of three sequence analysis based methods. Nucleic Acids Res. *34*, 1317–1325.
22. Ng, P.C., and Henikoff, S. (2003). SIFT: Predicting amino acid changes that affect protein function. Nucleic Acids Res. *31*, 3812–3814.
23. Ramensky, V., Bork, P., and Sunyaev, S. (2002). Human non-synonymous SNPs: Server and survey. Nucleic Acids Res. *30*, 3894–3900.
24. Guo, M., Ignatov, M., Musier-Forsyth, K., Schimmel, P., and Yang, X.L. (2008). Crystal structure of tetrameric form of human lysyl-tRNA synthetase: Implications for multisynthetase complex formation. Proc. Natl. Acad. Sci. USA *105*, 2331–2336.
25. Kovaleski, B.J., Kennedy, R., Hong, M.K., Datta, S.A., Kleiman, L., Rein, A., and Musier-Forsyth, K. (2006). In vitro characterization of the interaction between HIV-1 Gag and human lysyl-tRNA synthetase. J. Biol. Chem. *281*, 19449–19456.
26. Kunst, C.B., Mezey, E., Brownstein, M.J., and Patterson, D. (1997). Mutations in SOD1 associated with amyotrophic lateral sclerosis cause novel protein interactions. Nat. Genet. *15*, 91–94.
27. Nangle, L.A., Zhang, W., Xie, W., Yang, X.L., and Schimmel, P. (2007). Charcot-Marie-Tooth disease-associated mutant tRNA synthetases linked to altered dimer interface and neurite distribution defect. Proc. Natl. Acad. Sci. USA *104*, 11239–11244.
28. Delarue, M. (1995). Aminoacyl-tRNA synthetases. Curr. Opin. Struct. Biol. *5*, 48–55.
29. Hodapp, J.A., Carter, G.T., Lipe, H.P., Michelson, S.J., Kraft, G.H., and Bird, T.D. (2006). Double trouble in hereditary neuropathy: Concomitant mutations in the PMP-22 gene and another gene produce novel phenotypes. Arch. Neurol. *63*, 112–117.
30. Meggouh, F., de Visser, M., Arts, W.F., De Coo, R.I., van Schaik, I.N., and Baas, F. (2005). Early onset neuropathy in a compound form of Charcot-Marie-Tooth disease. Ann. Neurol. *57*, 589–591.
31. Chung, K.W., Sunwoo, I.N., Kim, S.M., Park, K.D., Kim, W.K., Kim, T.S., Koo, H., Cho, M., Lee, J., and Choi, B.O. (2005). Two missense mutations of EGR2 R359W and GJB1 V136A in a Charcot-Marie-Tooth disease family. Neurogenetics *6*, 159–163.
32. Seburn, K.L., Nangle, L.A., Cox, G.A., Schimmel, P., and Burgess, R.W. (2006). An active dominant mutation of glycyl-tRNA synthetase causes neuropathy in a Charcot-Marie-Tooth 2D mouse model. Neuron *51*, 715–726.
33. Rouleau, G.A., Merel, P., Lutchman, M., Sanson, M., Zucman, J., Marineau, C., Hoang-Xuan, K., Demczuk, S., Desmaze, C., Plougastel, B., et al. (1993). Alteration in a new gene encoding a putative membrane-organizing protein causes neuro-fibromatosis type 2. Nature *363*, 515–521.